Defect Aggregation in Anion-Excess Fluorites

II. Clusters Containing More than Two Impurity Atoms

P. J. BENDALL

Inorganic Chemistry Laboratory, South Parks Road, Oxford, United Kingdom

C. R. A. CATLOW

Department of Chemistry, University College London, London WC1H 0AJ, United Kingdom

J. CORISH*

Department of Chemistry, University College Dublin, Dublin 4, Ireland

AND P. W. M. JACOBS

Department of Chemistry, University of Western Ontario, London N6A 5B7, Ontario, Canada

A theoretical study has been made of defect clustering in fluorite crystals. The emphasis is on the aggregation processes that can occur beyond the dimer stage which was discussed previously (J. Corish, C. R. A. Catlow, P. W. M. Jacobs, and S. H. Ong, *Phys. Rev. B* **25,** 6425 (1982)). The systems studied comprise CaF_2, SrF_2, and BaF_2 doped with MF_3 where M = Y, Lu, Yb, Er, Tb, Gd, Eu, or La, and also $SrCl_2$ doped with $GdCl_3$, $LaCl_3$, or $PrCl_3$. Two tetramers, one containing a single anion vacancy and two $\langle 111 \rangle$ relaxed F^- ions and the other with a planar arrangement of the dopant ions, are stable for certain systems while a trimer and hexamers, with an octahedral arrangement of substitutional M^{3+}, also show considerable stability. A notable feature is the increase in the relative stability of larger complexes as the ratio of the radius of the dopant ion to that of the host lattice cation is decreased. The results are discussed in relation to recent EXAFS and neutron scattering work on these systems and should provide a useful guide in future experimental studies.

1. Introduction

The fluorite structure consists of a simple cubic array of fluoride ions with every alternate cube occupied by a divalent cation Ca, Sr, Ba, or Pb. It is this particular feature,

*To whom correspondence should be addressed at present address: Department of Chemistry, Trinity College, Dublin 2, Ireland.

namely, the existence of vacant cubic sites equal in number to the occupied cation sites, that enables crystals with the fluorite structure to accommodate a large number of anion interstitials. Thus the dominant intrinsic defects at high temperatures are anion Frenkel defects, while crystals with the fluorite structure have the property of forming a wide range of solid solutions with tri-

valent fluorides, MF_3. At low concentrations the M^{3+} ions substitute for the host-lattice divalent cations and charge compensation is effected by the inclusion of an equal number of anion interstitials. As the concentration of MF_3 is increased, these defects begin to cluster. The first-formed clusters are those which consist of a single M_s^{3+} ion and a single charge-compensating interstitial F^- in either the nearest neighbor (nn) or next-nearest neighbor (nnn) position, thus reducing the symmetry at the M_s^{3+} site from O_h to C_{4v} or C_{3v}, respectively. The next cluster to form is the dimer consisting of two M_s^{3+} and two F_i^-, either all on nn or all on nnn sites. This cluster is a particularly stable one and has the remarkable property of being able to trap a further interstitial F^- ion even if this has to be obtained by the dissociation of a monomer cluster or, in some substances, by migration from another dimer.

The stability of monomer and dimer clusters, and the reactions by which they form, have been discussed rather fully in a previous paper (*1*). In this paper we turn our attention to defect clusters containing more than two impurity atoms. The systems investigated are broadly the same as in Ref. (*1*), namely, CaF_2, SrF_2, and BaF_2 containing Y^{3+} and the trivalent rare-earth ions Lu^{3+}, Yb^{3+}, Er^{3+}, Tb^{3+}, Gd^{3+}, Eu^{3+}, and La^{3+}; though complete results are not always available for every system, they are sufficient to establish trends in stability. Apart from the neutron diffraction and EXAFS studies to be discussed later in this paper, there is experimental evidence for the existence of clusters containing more than two impurity atoms. Andeen et al. (*2*) have associated their R_{III} relaxation, which dominates the plot of ε'' vs T for small rare earths, with either a higher-order complex (trimer) or a superstructure, and Seelbinder and Wright (*3*) have observed three-body energy transfer, following laser excitation, which demonstrates that there are clusters

in CaF_2 which contain at least three lanthanide ions. In addition we have also considered $SrCl_2$ doped with Gd^{3+}, Pr^{3+}, and La^{3+}. Our present technique for calculating defect energies involves calculating the energy of a crystal that contains a single cluster. It is therefore not appropriate for the study of the onset of superstructure phases, like those that have been studied extensively by Greiss (*4–7*) and also by Fedorov et al. (*8, 9*) and Tkachenko et al. (*10*). We reserve the theoretical study of these superstructure phases to a subsequent paper.

2. Method of Calculation

We use the now-standard computer simulation procedure as programmed in the HADES code (*11, 12*). The technique is based on the familiar Mott–Littleton approach in which the simulated crystal consists of two regions, an inner region containing the defect in which the ions are specifically relaxed and an outer region which is treated as a dielectric continuum. The inner regions were carefully chosen to include complete symmetry classes and

TABLE I

INTERIONIC POTENTIALS FOR THE $SrCl_2$ SYSTEMS

(a) The form of the short range potentials is $\phi(r) = A \exp(-r/\rho)$

Interaction	A (eV)	ρ (Å)
Sr^{2+}–Cl^-	2250.3	0.3397
Cl^-–Cl^-	1227.18	0.3214
Cl^-–Gd^{3+}	1830.18	0.3005
Cl^-–La^{3+}	2624.46	0.3384
Cl^-–Pr^{3+}	2580.50	0.3394

(b) Shell constants for ions of the host crystal

	Y ($|e|$)	k (eV Å^{-2})
Sr^{2+}	5.0378	111.96
Cl^-	−2.519	35.985

Note. The impurity ions were given the same shell constants as the Sr^{2+} ion.

TABLE II

NOTATION FOR DEFECTS AND DEFECT
CLUSTERS IN FLUORITE CRYSTALS

Description	Notation
Isolated vacancy	0|1|0|0
Free interstitial	0|0|0|1
Substitutional impurity	1|0|0|0
nn monomer	1|0|0|1_1
nnn monomer	1|0|0|1_2
Dimer	2|0|2|2_1
Trimer	3|0|1|3_1
Tetramers	4|1|2|4_1; 4|0|8|4_1
Ionized hexamers	6|0|8|4_1; 6|0|8|5_1
Neutral hexamers	6|0|8|$6_1{}^a$

Note. The trimer, tetramers, and hexamers
are illustrated in Figs. 1–7.

^{a} These are of two types, depending on
whether two of the relaxed lattice ions are
aligned along $\langle 100 \rangle$ or $\langle 111 \rangle$ directions. This will
be indicated by appending the symbol showing
the orientation of the relaxed ions.

generally contained at least 125 ions. In certain calculations the size of the inner region was much larger and contained up to 400 ions. The minimization step which establishes the equilibrium positions of the ions in both regions therefore required a very large amount of computer core. Our calculations are therefore confined to the harmonic approximation but it is not expected that this limitation would affect our general conclusions as to the stability of the various defect clusters. The interionic potentials for CaF_2, SrF_2, and BaF_2 were the same as those employed previously (*1*). Those for $SrCl_2$ are given in Table I and are based on those derived by Bendall (*13*).

3. Results and Discussion

The notation used to describe the defect clusters is an extension of that introduced in Ref. (*1*). A cluster is described by the symbol $i|v|p|q_r s_t \ldots$, where i denotes the number of trivalent substitutional impurity ions, v the number of vacancies, p the number of relaxed lattice ions, q the number of interstitials in nn sites ($r = 1$), and s the number of interstitials in nnn sites ($t = 2$). We should emphasize here that this notation distinguishes between a vacancy and a vacant site which results from relaxation of that lattice ion. Thus in accordance with the convention used in Ref. (*1*), relaxed lattice ions are *not* considered as separate vacancies and interstitials but rather as vacancy–interstitial pairs. Previously, their number was not noted explicitly; but it is clear that this is somewhat disadvantageous when describing larger clusters as the former notation does not then describe adequately the structure of the cluster. A summary of the defects and defect clusters considered is given in Table II. The monomers and dimers were illustrated in Ref. (*1*); the trimer, two tetramers, and four hexamers are shown in Figs. 1–7. The origin of the coordinate system is taken at an interstitial site and the lattice parameter is the shortest anion–anion distance.

A particular calculation yields the energy of the (relaxed) defect configuration under consideration. What is of primary interest, however, is the energy of this configuration
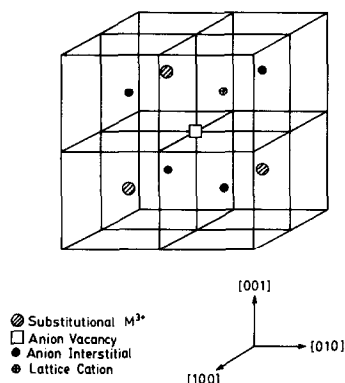

⊘ Substitutional M^{3+}
□ Anion Vacancy
● Anion Interstitial
⊕ Lattice Cation

[001]
[010]
[100]

FIG. 1. The 3\|0\|1\|3_1 trimer containing three M_s^{3+} impurity ions, three charge-compensating anion interstitials, and one relaxed lattice ion in a $\langle 1\bar{1}1 \rangle$ direction. The directions of the axes used in the calculations and for all the figures are also shown.
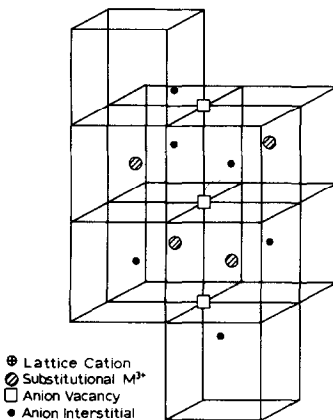
FIG. 2. The $4|1|2|4_1$ tetramer containing four M_s^{3+} impurity ions, four charge-compensating anion interstitials, and two relaxed lattice ions in $\langle 111 \rangle$ directions that will enhance Coulomb interactions with M_s^{3+} ions. The cluster is stabilized by the presence of a central anion vacancy. (This is the same cluster as the one formerly termed $3:4:2$.)

relative to that of other possible clusters containing the same number of primary defects, substitutional impurity ions, vacancies, and interstitials. The results given in the tables are therefore the energies associated with the formation of the defect cluster concerned by the re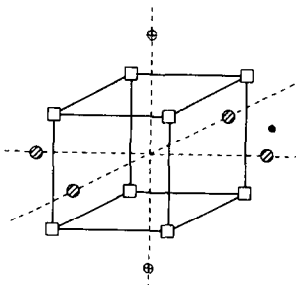action given in Table III. The usefulness of the notation employed is at once apparent since the numbers of primary defects must balance in any reaction. The necessity for distinguishing vacancy–interstitial pairs that are relaxed lattice ions is also apparent since these conserve mass and structure internally and do not need to balance on each side of the quasichemical equations in Table III. All the energies given in Tables IV–IX are normalized to one M_s^{3+}. Thus, for example, the first entry in the third row of Table IV tells us that the nn dimer is more stable than two separated nn monomers in CaF_2: Y^{3+} by 0.298 eV per Y^{3+}. The reason for quoting the energies of formation of monomers and dimers (from monomers) when this information is already available in Ref. (*1*) is that the tables provide a complete picture of the association of M_s^{3+} and interstitials to form clusters in the systems under consideration. It is possible then to see at a glance which clusters are likely to be present in each mixed-crystal system. Some cautionary notes must, however, be stated. It must be emphasized that the energy changes calculated are constant-volume energies and not Helmholtz' or Gibbs' energies so that any predictions of stability of the clusters will be affected by the corresponding en-

FIG. 3. The $4|0|8|4_1$ tetramer containing 4 M_s^{3+} impurity ions at (± 1, 0, 0), 8 anion vacancies situated at ($\pm\frac{1}{2}$, $\pm\frac{1}{2}$, $\pm\frac{1}{2}$) and 12 interstitials, initially at (± 1, ± 1, 0). Only *one* of these interstitials is shown for reasons of clarity. The interstitials relax considerably toward the two nearest impurity ions (or one impurity and one host cation) in order to increase Coulombic interactions and stabilize the cluster.

TABLE III

CLUSTER REACTIONS LEADING TO
THE FORMATION OF DEFECT
CLUSTERS IN FLUORITE CRYSTALS

(1) $1|0|0|0 + 0|0|0|1 = 1|0|0|1_1$
(2) $2(1|0|0|1_1) = 2|0|2|2_1$
(3) $2(2|0|2|2_1) = 4|1|2|4_1 + 0|0|0|1$
(4) $2(2|0|2|2_1) = 4|0|8|4_1$
(5) $3(2|0|2|2_1) = 6|0|8|4_1 + 2(0|0|0|1)$
(6) $3(2|0|2|2_1) = 6|0|8|5_1 + \quad 0|0|0|1$
(7) $3(2|0|2|2_1) = 6|0|8|6_1 \quad \langle 100 \rangle$
(8) $3(2|0|2|2_1) = 6|0|8|6_1 \quad \langle 111 \rangle$
(9) $2|0|2|2_1 + 1|0|0|1_1 = 3|0|1|3_1$

Note. The notation used is explained in the text and the defect clusters are described briefly in Table II.

TABLE IV

ENERGY CHANGES[a] ON FORMING DEFECT CLUSTERS IN CaF_2 BY THE REACTION SHOWN

Reaction:	1	2	3	4	5	6	7	8
Cluster:	$1\|0\|0\|1_1$	$2\|0\|2\|2_1$	$4\|1\|2\|4_1$	$4\|0\|8\|4_1$	$6\|0\|8\|4_1$	$6\|0\|8\|5_1$	$6\|0\|8\|6_1$ $\langle100\rangle$	$6\|0\|8\|6_1$ $\langle111\rangle$
Y^{3+}	−0.502	−0.298	−0.171	−0.628	−0.292	−0.696	−0.359	−0.691
Lu^{3+}	−0.710	−0.173	−0.248		+0.242	−0.284	−0.073	−0.438
Yb^{3+}	−0.706	−0.212	−0.264	−0.124	+0.206	−0.319	−0.076	−0.437
Er^{3+}	−0.730	−0.176	−0.258		+0.279	−0.258	−0.036	−0.431
Tb^{3+}	−0.708	−0.159	−0.240	−0.083	+0.227	−0.265	−0.045	−0.414
Gd^{3+}	−0.713	−0.164	−0.244	−0.081	+0.261	−0.267	−0.046	−0.420
Eu^{3+}	−0.765	−0.154	−0.260		+0.378	−0.179	+0.021	−0.373
La^{3+}	−0.799	−0.210	−0.184	+0.195	+0.547	−0.194	+0.152	−0.242

[a] In eV per one M_s^{3+} ion.

TABLE V

ENERGY CHANGES[a] ON FORMING DEFECT CLUSTERS IN SrF_2 BY THE REACTION SHOWN

Reaction:	1	2	3	4	5	6	7	8
Cluster:	$1\|0\|0\|1_1$	$2\|0\|2\|2_1$	$4\|1\|2\|4_1$	$4\|0\|8\|4_1$	$6\|0\|8\|4_1$	$6\|0\|8\|5_1$	$6\|0\|8\|6_1$ $\langle100\rangle$	$6\|0\|8\|6_1$ $\langle111\rangle$
Y^{3+}	−0.401	−0.200	+0.004	−0.672	−0.341	−0.586	−0.395	−0.567
Lu^{3+}	−0.524	−0.126	−0.101		−0.048	−0.388	−0.247	−0.497
Yb^{3+}	−0.509	−0.159	−0.101	−0.331	−0.027	−0.412	−0.248	−0.528
Er^{3+}	−0.535	−0.131	−0.112		−0.029	−0.376	−0.232	−0.498
Tb^{3+}	−0.527	−0.114	−0.102	−0.290	−0.034	−0.378	−0.244	−0.482
Gd^{3+}	−0.529	−0.119	−0.104	−0.291	−0.035	−0.378	−0.243	−0.486
Eu^{3+}	−0.563	−0.114	−0.131		+0.030	−0.333	−0.204	−0.474
La^{3+}	−0.592	−0.099	−0.145	−0.150	+0.089	−0.293	−0.176	−0.450

[a] In eV per one M_s^{3+} ion.

TABLE VI

ENERGY CHANGES[a] ON FORMING DEFECT CLUSTERS IN BaF_2 BY THE REACTION SHOWN

Reaction:	1	2	3	4	5	6	7	8
Cluster:	$1\|0\|0\|1_1$	$2\|0\|2\|2_1$	$4\|1\|2\|4_1$	$4\|0\|8\|4_1$	$6\|0\|8\|4_1$	$6\|0\|8\|5_1$	$6\|0\|8\|6_1$ $\langle100\rangle$	$6\|0\|8\|6_1$ $\langle111\rangle$
Y^{3+}	−0.376	ED						
Lu^{3+}	−0.369	−0.239	+0.092		−0.040	−0.184	PPC	−0.199
Yb^{3+}	−0.344	−0.236	+0.082	−0.241	−0.093	−0.228	ED	−0.240
Er^{3+}	−0.372	−0.228	+0.076		−0.049	−0.196	ED	−0.221
Tb^{3+}	−0.380	−0.242	+0.086	−0.154	−0.015	−0.163	ED	−0.176
Gd^{3+}	−0.379	−0.239	+0.084	−0.164	−0.024	−0.158	ED	−0.189
Eu^{3+}	−0.397	−0.211	+0.072		−0.017	−0.179	PPC	−0.224
La^{3+}	−0.423	−0.141	−0.005	−0.154	−0.040	−0.215	ED	−0.278

Note. The symbols ED (excessive displacement of lattice ions) and PPC (persistent positive curvature of the energy surface) indicate that a stable configuration could not be located.
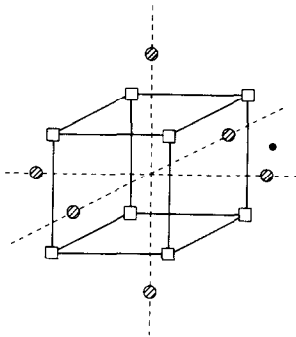
[a] In eV per one M_s^{3+} ion.

FIG. 4. The $6|0|8|4_1$ hexamer. This is derived from the $4|0|8|4_1$ cluster by adding two more substitutional impurity ions at $(0, 0, \pm 1)$ and consequently has a net charge of $+2$.

FIG. 6. In the first of the $6|0|8|6_1$ hexamers there are two additional interstitials aligned along $\langle 100 \rangle$.

tropy changes. There is very little information available on these entropy changes except for the formation of monomers from isolated M_s^{3+} and interstitials, where Δs is normally negative and of the order of $1-3k$. If the vibrational entropy changes per M_s^{3+} ion continue to be of that order then any conclusions as to stability of defect clusters that are based on energy changes of several tenths of an electron volt will not be affected. Another point to be borne in mind is that the actual cluster concentrations will depend not only on the equilibrium constants but on the concentrations (strictly, activities) of the reactants and hence pri-

marily on the concentration of MF_3 present in the crystal. Thus, at low concentrations one will expect the small clusters to predominate, while at higher concentrations there will be a greater tendency to form the stable large clusters. With these points in mind we proceed to analyze the results in Tables IV–IX.

Table IV shows the results for CaF_2. The energies of reactions 1–3 emphasize the stabilities of monomer, dimer, and the tetramer stabilized by the central vacancy (Fig. 2). Generally, the most stable hexamers to be expected in CaF_2 are the $6|0|8|5_1$ cluster (Fig. 5) and the $6|0|8|6_1$ cluster where two of the relaxed lattice ions form a $\langle 111 \rangle$ oriented "dumbell" about the center of the cluster (Fig. 7). However, Y^{3+} clearly has a tremendous ability to form clusters of almost every kind—a feature which may be
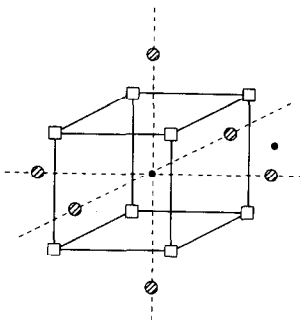

FIG. 5. In the $6|0|8|5_1$ hexamer, one of the excess positive charges of the $6|0|8|4_1$ cluster is neutralized by an additional interstitial at the origin.
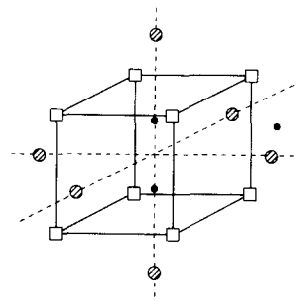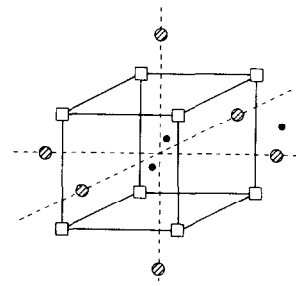

FIG. 7. In the second type of $6|0|8|6_1$ hexamer the two extra interstitials are aligned along $\langle 111 \rangle$.

TABLE VII

ENERGY CHANGES[a] ON FORMING DEFECT CLUSTERS IN BaF_2

Reaction: Cluster:	1' $1\|0\|0\|1_2$	2' $2\|0\|2\|2_2$	3' $4\|1\|2\|4_1$	4' $4\|0\|8\|4_1$	5' $6\|0\|8\|4_1$	6' $6\|0\|8\|5_1$	8' $6\|0\|8\|6_1$ $\langle 111 \rangle$
Y^{3+}	−0.626	−0.231	ED	−0.134	+0.102	+0.015	+0.135
Lu^{3+}	−0.567	−0.210	+0.511		+0.129	−0.015	−0.030
Er^{3+}	−0.565	−0.210	+0.252		+0.127	−0.021	−0.046
Gd^{3+}	−0.568	−0.207	+0.215	−0.031	+0.133	−0.040	−0.035
Eu^{3+}	−0.555	−0.204	+0.214		+0.134	−0.028	−0.073
La^{3+}	−0.546	−0.197	+0.175	−0.099	+0.139	−0.036	−0.099

Note. The primed reactions are the same as the unprimed ones in Table 3, except that the monomers and dimers contain interstitials that occupy sites that are second neighbors to the impurity cations.

[a] In eV per one M_s^{3+} ion.

related to its small ionic radius which allows extensive relaxation of the dopant ion.

Results for SrF_2 are given in Table V. Again the larger Y^{3+} clusters investigated are especially stable. In all the tables Y^{3+} (which has no f electrons) occupies first place in the list of substituents and thereafter the rare-earth ions follow in order of increasing ionic radius R. Whereas the overall trend in the stability of the rare-earth dimers is to show a decrease with increasing R, the stability of $4\|1\|2\|4_1$ clusters increases with increasing R, though the effect is not large. In contrast the stability of $4\|0\|8\|4_1$ clusters decreases with increasing R as shown by the decrease in their formation energy from dimers of more than 50% from Yb^{3+} to La^{3+}. In SrF_2 (except for Y^{3+}) the hexamer with two excess positive charges and two compensating free interstitials (see reaction 5) has about the same stability as three separate dimers. However, the addition of a central interstitial during clustering (reaction 6) or of two $\langle 100 \rangle$ or $\langle 111 \rangle$ interstitials (reactions 7 and 8) stabilizes the hexamer cluster. Thus in SrF_2 we may expect to see nn (and also nnn (*1*)) monomers, dimers, tetramers, and a variety of hexamers, except the doubly charged $|6\|0\|8\|4_1$.

In BaF_2 the nn Y^{3+} dimer $2\|0\|2\|2_1$ displayed an excessive displacement of lattice

ions during minimization, indicative of some instability in the system. For the rare-earth ions the monomers, dimers, and $4\|0\|8\|4_1$ tetramers are all stable. As in SrF_2, the doubly positive charged $6\|0\|8\|4_1$, plus two charge-compensating free interstitials, have about the same stability as three dimers. The $6\|0\|8\|6_1$ hexamer with two $\langle 100 \rangle$ interstitials is clearly an unstable configuration in BaF_2 since in two cases no minimum could be found and in the remaining five cases excessive displacement of lattice ions occurred. The hexamers with one central interstitial, or two interstitials aligned along $\langle 111 \rangle$, are both stable with respect to three nn dimers. In BaF_2 the nnn monomers and dimers are more stable than their nn counterparts. Therefore it is necessary to see if the nnn dimer is the terminal cluster in the aggregation process in BaF_2. Table VII shows the stability of the higher clusters with respect to the $2\|0\|2\|2_2$ nnn dimer and it is clear that the tetramers and hexamers are unlikely to form extensively from nnn dimers. This is not to say that they may not be found to exist in BaF_2 for the energy changes for reactions 4', 6' and 8', though small, are mostly slightly negative. Thus the higher clusters will exist in equilibrium with the nnn monomers and dimers.

Table VIII shows corresponding results

BENDALL ET AL.

TABLE VIII

Energy Changes[a] on Forming Defect Clusters in $SrCl_2$ from nn and nnn Monomers and Dimers by the Reaction Shown

Cluster:	$1\|0\|0\|1_1$	$2\|0\|2\|2_1$	$4\|1\|2\|4_1$	$4\|0\|8\|4_1$	$6\|0\|8\|4_1$	$6\|0\|8\|5_1$	$6\|0\|8\|6_1$ $\langle 100 \rangle$	$6\|0\|8\|6_1$ $\langle 111 \rangle$
Reaction:	1	2	3	4	5	6	7	8
Gd^{3+}	(−0.924)	−1.573	ED	−0.150	+0.980	+1.400	−0.954	ED
Pr^{3+}	−0.327	−0.273	+0.011	−0.391	−0.123	−0.378	−0.257	−0.484
La^{3+}	−0.328	−0.273	+0.012	−0.390	−0.123	−0.378	−0.256	−0.484
Reaction:	1′	2′	3′	4′	5′	6′	7′	8′
Gd^{3+}	−3.410	+1.569	ED	−0.085	+1.108	+1.529	−0.826	ED
Pr^{3+}	−0.439	−0.142	−0.009	−0.410	−0.142	−0.397	−0.276	−0.503
La^{3+}	−0.438	−0.142	−0.176	−0.410	−0.143	−0.398	−0.276	−0.505

[a] In eV per one M_s^{3+} ion.

for three dopants in $SrCl_2$. For La^{3+} and Pr^{3+} all the clusters examined are stable. The behavior of Gd^{3+} is exceptional and attempts to model this system proved to be more difficult than expected. The nn monomer and dimer and the nnn dimer are, in general, exceptionally stable and there is little tendency to form higher complexes except the $\langle 100 \rangle$ hexamer. The ion movements in $SrCl_2$: Gd^{3+} are exceptionally large (Tables IX and X) due to the large differences in the ion sizes of Gd^{3+} and

TABLE IX

Energy Changes[a] on Forming Trimer Clusters in CaF_2, SrF_2, and BaF_2 from a Monomer and a Dimer, According to Reaction 9

M^{3+}	CaF_2	SrF_2	BaF_2
Y^{3+}	−0.545	−0.292	[b]
Yb^{3+}	−0.583	−0.402	−0.202
Tb^{3+}	−0.509	−0.333	−0.193
Gd^{3+}	−0.518	−0.374	−0.197
La^{3+}	−0.479	−0.405	−0.272

[a] In eV per one M_s^{3+} ion.
[b] The energy of formation of the dimer could not be found for BaF_2: Y^{3+}.

TABLE X

Ion Positions in the Minimum Energy Configuration of the $6\|0\|8\|5_1$ Cluster (Fig. 5)

System	x	
	6 impurity ions relaxed from (1.0, 0, 0) to $(x, 0, 0)$	12 F^- interstitials relaxed from (0.8, 0.8, 0) to $(x, y = x, 0)$
CaF_2: Y^{3+}	1.042	0.730
CaF_2: Yb^{3+}	1.065	0.755
CaF_2: Tb^{3+}	1.068	0.759
CaF_2: Gd^{3+}	1.068	0.759
CaF_2: La^{3+}	1.076	0.769
SrF_2: Y^{3+}	0.999	0.703
SrF_2: Yb^{3+}	1.024	0.726
SrF_2: Tb^{3+}	1.028	0.731
SrF_2: Gd^{3+}	1.029	0.731
SrF_2: La^{3+}	1.037	0.740
BaF_2: Y^{3+}	0.964	0.642
BaF_2: Yb^{3+}	0.995	0.674
BaF_2: Tb^{3+}	1.000	0.677
BaF_2: Gd^{3+}	0.999	0.677
BaF_2: La^{3+}	1.009	0.688
$SrCl_2$: Gd^{3+}	1.298	0.776
$SrCl_2$: Pr^{3+}	1.020	0.739
$SrCl_2$: La^{3+}	1.020	0.739

Note. The central F^- interstitial at the origin is fixed by symmetry.

Sr^{2+}. The available experimental binding energies of Gd^{3+} with an interstitial chloride ion are large (14) and similar large dopant-defect binding energies have been found in other systems where there is a large difference between the radii of the dopant and lattice ion; a good example is provided by $CeO_2 : Sc^{3+}$ (15).

The energies of formation of trimer clusters (Fig. 1) in CaF_2, SrF_2, and BaF_2 from a monomer and a dimer (reaction 9 of Table III) are given in Table IX. These results show that the trimer is very stable in CaF_2, less so in SrF_2 and less so again in BaF_2. This dependence of cluster stability on lattice constant occurs because a small lattice constant increases the Coulomb interactions between impurity ions and interstitials and thus enhances the stability of the smaller clusters (cf. the monomer stabilities in Tables IV–VI). Because the trimer is

more stable than the tetramer in CaF_2 (except for the anomalous case of Y^{3+} already referred to) it is interesting to speculate that in CaF_2 the formation of hexamers might involve the aggregation of two trimers, accompanied by the relaxation of six lattice F^- ions, rather than the dimer $\rightarrow$ tetramer $\rightarrow$ hexamer route. However, for SrF_2 and BaF_2 both intermediates, trimer and tetramer, have about the same stability.

The HADES program provides detailed information on the position of every ion in the calculation. It is obviously impossible to reproduce all of this information here but the positions of the ions in the cluster in the lowest energy configurations are shown in Tables X and XI for the two most stable hexamers, $6|0|8|5_1$ (Fig. 4) and $6|0|8|6_1$ $\langle 111 \rangle$ (Fig. 7). The impurity ions were found to remain within 8% of their initial positions at $(1.0, 0, 0)$ with the exception of Gd^{3+} in

TABLE XI

Ion Positions in the Minimum Energy Configuration of the $6|0|8|6_1$ Cluster (Fig. 7)

System	6 impurity ions relaxed from (1.0, 0, 0) to $(x, y, z = y)$		6 F^- interstitials relaxed from (0.8, 0.8, 0) to $(x, y = x, z)$		6 F^- interstitials from $(-0.8, 0.8, 0)$ to $(x, y = x, 0)$	2 F^- interstitials relaxed from lattice sites at (0.5, 0.5, 0.5) to $(x, y = x, z = x)$
	x	y	x	z	x	x
$CaF_2 : Y^{3+}$	1.019	0.023	0.822	−0.011	−0.714	0.171
$CaF_2 : Yb^{3+}$	1.079	0.022	0.826	−0.195	−0.713	0.244
$CaF_2 : Tb^{3+}$	1.045	0.023	0.849	−0.015	−0.743	0.184
$CaF_2 : Gd^{3+}$	1.047	0.023	0.849	−0.014	−0.742	0.184
$CaF_2 : La^{3+}$	1.055	0.024	0.857	−0.014	−0.752	0.188
$SrF_2 : Y^{3+}$	0.972	0.028	0.786	−0.002	−0.680	0.168
$SrF_2 : Yb^{3+}$	1.002	0.027	0.811	−0.007	−0.703	0.187
$SrF_2 : Tb^{3+}$	1.008	0.026	0.817	−0.009	−0.710	0.190
$SrF_2 : Gd^{3+}$	1.008	0.028	0.816	−0.008	−0.709	0.190
$SrF_2 : La^{3+}$	1.017	0.026	0.824	−0.010	−0.719	0.195
$BaF_2 : Y^{3+}$	0.946	0.008	0.746	−0.103	−0.612	0.211
$BaF_2 : Yb^{3+}$	0.978	0.020	0.771	−0.074	−0.640	0.227
$BaF_2 : Tb^{3+}$	0.985	0.019	0.778	−0.080	−0.646	0.231
$BaF_2 : Gd^{3+}$	0.984	0.019	0.777	−0.080	−0.645	0.230
$BaF_2 : La^{3+}$	0.994	0.020	0.785	−0.079	−0.656	0.235
$SrCl_2 : Gd^{3+}$	1.268	0.134	0.843	−0.171	−1.065	0.376
$SrCl_2 : Pr^{3+}$	0.990	0.028	0.812	−0.008	−0.720	0.163
$SrCl_2 : La^{3+}$	0.990	0.028	0.812	−0.008	−0.720	0.163

$SrCl_2$ which shows a pronounced outward relaxation at almost 30%. The 12 symmetrical interstitials of the $6|0|8|5_1$ cluster all move in from their initial placing at (0.8, 0.8, 0). The extent of this movement is related to the ion radius of the dopant and the lattice parameter of the host. The smaller the trivalent ion the further the movement of the F^- interstitials. This inward movement is also facilitated by an increase in the lattice parameter. The closer the approach of the interstitials to the trivalent ions the greater is the stabilization of the cluster by their Coulomb interaction. The same general principles obtain for the 12 analogous interstitials of the $6|0|8|6_1$ cluster although they are not now constrained by symmetry to be a single set. The two ⟨111⟩ interstitials move inward from their initial lattice positions at (0.5, 0.5, 0.5).

The most significant overall trend in the results is for increased stability of the large clusters, involving an octahedron of M^{3+} ions, compared with the smaller dopant dimers and tetramers (the $2|0|2|2_1$ and $4|1|2|4_1$ clusters) on increasing the ratio of the lattice parameter to the radius of the dopant ion. Recent experimental evidence from neutron diffraction and EXAFS studies supports this prediction. Single-crystal Bragg diffraction experiments have been carried out on $CaF_2 : La^{3+}$ (16, 17) $CaF_2 : Er^{3+}$ (17, 18), and $SrCl_2 : Pr^{3+}$ (19). In the first system a dopant dimer appears to be present, whereas the results for the $CaF_2 : Er^{3+}$ and $SrCl_2 : Pr^{3+}$ systems suggest the presence of the octahedral clusters. We note that the ionic radius of Er^{3+} is less than that of La^{3+}, and that the lattice parameter of $SrCl_2$ is greater than that of CaF_2. The EXAFS studies (20, 21) on $CaF_2 : La^{3+}$ and $CaF_2 : Er^{3+}$ are in line with the results of the neutron diffraction measurements. A distinct difference is noted between the EXAFS spectra of the rare earths in the two systems; and while the former spectrum can be explained adequately by clus-

ter models based on dopant dimers and monomers, the latter is compatible with the octahedral cluster models.

4. Conclusions

This continuation of our earlier work (1) shows that fluorite systems containing M^{3+} are further stabilized when the monomers and dimers aggregate to form larger clusters. In assessing the relative stabilities of different aggregates in a number of systems effects due to host lattice parameter and impurity ion radius are evident: increasing the ratio of the lattice parameter to the radius of the dopant ion increases the stability of the hexamers with an octahedron of M^{3+} ions. Crystals which contain these clusters would be expected to show little evidence of ⟨111⟩ interstitials and this prediction is in line with neutron diffraction and EXAFS measurements.

References

1. J. CORISH, C. R. A. CATLOW, P. W. M. JACOBS, AND S. H. ONG, *Phys. Rev. B* **25**, 6425 (1982).
2. C. G. ANDEEN, J. J. FONTANELLA, M. C. WINTERSGILL, P. J. WELCHER, R. J. KIMBLE, AND G. E. MATTHEWS, *J. Phys. C* **14**, 3557 (1981).
3. M. B. SEELBINDER AND J. C. WRIGHT, *J. Chem. Phys.* **75**, 5070 (1981).
4. O. GREIS, *J. Solid State Chem.* **24**, 227 (1978).

5. O. GREIS, *Z. Anorg. Allg. Chem.* **434,** 89 (1977).

6. D. J. M. BEVAN AND O. GREIS, *Rev. Chim. Miner.* **15,** 346 (1978).

7. O. GREIS, "The Rare Earths in Modern Science and Technology," Vol. II, Plenum, New York (1979).

8. P. P. FEDOROV, O. E. IZATOVA, V. B. ALEXANDROV, AND B. P. SOBOLEV, *J. Solid State Chem.* **9,** 368 (1974).

9. B. P. SOBOLEV AND P. P. FEDOROV, *J. Less-Common Met.* **60,** 35 (1978).

10. N. L. TKACHENKO, L. S. GARASHINA, O. E. IZOTOVA, V. B. ALEKSANDROV, AND B. SOBOLEV, *J. Solid State Chem.* **8,** 213 (1973).

11. M. J. NORGETT, AERE Harwell Report R7650, 1974.

12. C. R. A. CATLOW AND W. C. MACKRODT, *in* "Computer Simulation of Solids" (C. R. A. Catlow and W. C. Mackrodt, Eds.), Lecture Notes in Physics, Vol. 166, Springer-Verlag, Belin (1982).

13. P. J. BENDALL, D. Phil. thesis, Oxford (1980).

14. A. V. CHADWICK, F. G. KIRKWOOD, AND R. SAGHAFIAN, *J. Phys.* **41,** C6-216 (1980).

15. R. GERHARDT-ANDERSON AND A. S. NOWICK, *Solid State Ionics* **5,** 547 (1981).

16. C. R. A. CATLOW, A. V. CHADWICK, AND J. CORISH, *J. Solid State Chem.* **48,** 65 (1983).

17. C. R. A. CATLOW, A. V. CHADWICK, AND J. CORISH, *Radiat. Effects* **75,** 61 (1983).

18. C. R. A. CATLOW, A. V. CHADWICK, AND J. CORISH, to be published.

19. P. J. BENDALL, C. R. A. CATLOW, AND B. E. F. FENDER, *J. Phys. C,* in press.

20. C. R. A. CATLOW, L. M. MORONEY, A. V. CHADWICK, AND G. N. GREAVES, *Radiat. Effects* **75,** 61 (1983).

21. L. M. MORONEY, C. R. A. CATLOW, A. V. CHADWICK, AND G. N. GREAVES, *in* "EXAFS and Near-Edge Structure" (A. Bianconi, L. Incoccia, and S. Stipcich, Eds.), Springer-Verlag, Berlin, in press.